Building Serv. Eng. Res. Technol. 14(4) 151–157 (1993) Printed in Great Britain

Summary A new method for modelling multi-zone air infiltration and ventilation simulation and a simple test case are described. The network approach was used, and the solution was based on a fully implicit formulation of the flow equations. In the present version of the building simulation model (BUS version 2.1), the thermal behaviour of a building is neglected, and constant and uniform air temperatures are assumed. Convergence of the program was tested by test runs. The simulated steady-state mass flow rates and pressures were checked by analytical calculations. The results are found to satisfy both mass balance equations for every node and momentum equations for each flow element when a simple test case is simulated.

New building air flow simulation model: Theoretical basis

P Tuomaala MSc LicTech
Laboratory of Applied Thermodynamics, Helsinki University of Technology, Otakaari 4A (K1) SF-02150 Espoo, Finland

Received 9 November 1992, in final form 10 March 1993

List of symbols

a_0 Parameter for polynomic flow element (Pa)
a_1 Parameter for polynomic flow element (Pa kg^{-1} s)
a_2 Parameter for polynomic flow element (Pa kg^{-2} s^2)
a_{quadr} Parameter for quadratic flow element (Pa m^{-3} s)
A_{ij} Area of the flow element between nodes i and j (m^2)
b_{quadr} Parameter for quadratic flow element (Pa m^{-6} s^2)
C_p Wind pressure coefficient
C_{plc} Pressure loss coefficient of a power law flow element (Pa m^{3n} s^n)
d_{ij} Diameter of the flow element between nodes i and j (m)
h_i Height of an opening from node level (m)
K_{ij} Dynamic pressure loss coefficient between nodes i and j (Pa kg^{-2} s^2)
L_{ij} Length of the flow element between nodes i and j (m)
$\dot{m}_{ij}$ Mass flow rate between nodes i and j (kg s^{-1})
p_i Pressure in node i (Pa)
R_i Mass balance residual in node i (kg s^{-1})
R_{ij}^m Momentum equation residual of a flow element (Pa)
s_0 Parameter value for fan pressure curve fitting (Pa)
s_1 Parameter value for fan pressure curve fitting (Pa m^{-3} s)
s_2 Parameter value for fan pressure curve fitting (Pa m^{-6} s^2)
s_3 Parameter value for fan pressure curve fitting (Pa m^{-9} s^3)
S_i Mass flow rate source in node i (kg s^{-1})
S_{ij} Pressure source in flow element between nodes i and j (Pa)
t Time (s)
v Flow velocity (m s^{-1})
V_i Volume of node i (m^3)
$\dot{V}_{ij}$ Volumetric flow rate between nodes i and j (m^3 s^{-1})
z Level of a node from reference (m)
δ Damper opening angle (°)
λ Friction loss coefficient
ρ Density (kg m^{-3})
ζ Pressure loss coefficient
$\Delta\dot{m}_{ij}$ Mass flow rate correction during an iteration loop (kg s^{-1})
Δp Pressure difference across a flow element (Pa)
Δp_i Pressure correction during an iteration loop (Pa)

1 Introduction

Air infiltration and ventilation have a strong impact on both the indoor air quality and energy consumption in buildings. Therefore, it is important from the epidemiological and energy conservation points of view to be able to investigate and predict the behaviour of an air infiltration and ventilation process as effectively and reliably as possible.

There are two main strategies to study the behaviour of a process: experimental investigation and theoretical calculations. Experimental investigation of full-scale buildings is usually extremely expensive because of high investment costs and the need for complex instrumentation. The experimental investigation of buildings using small-scale models also easily becomes relatively expensive and difficult to perform.

By using theoretical calculations, at least some of the disadvantages mentioned above can be avoided. Simulation calculations are relatively cheap to perform in proportion to building costs. The calculation results of simulation programs can be obtained independently of external factors (e.g. outdoor air temperature variation), and any combination of these factors can be selected and given freely as input parameters to a simulation program. Sometimes a very important issue is that the theoretical calculations can also be performed independently of time (e.g. the annual energy consumption of a building can be calculated in a much shorter period of time than the measurements would take). Perhaps the greatest advantage of the theoretical calculations, however, is the completeness of the information they produce on the simulated process. This means that all of the calculated values of the variables are available for further investigation of the process. This is an important advantage compared, for example, with experimental investigation of the process, when every important location of the process (i.e. the placement of measuring devices) needs to be decided beforehand, and not all the information about the process is obtainable because of its complexity and the disturbance caused by the measuring devices.

Theoretical calculations naturally have their own disadvantages. Very complex processes are very difficult: to calculate, and they consume resources. These problems can be solved by simplifying the process to be simulated, but this simplification can become an essential source of errors. Sometimes a more harmful feature is that not all physical phenomena have yet been modelled with reasonable confidence (e.g. turbulence effect of air flow). Selection of a prediction method depends strongly on the nature and dominant physical phenomena of the process. When investigating a ventilation process, the only reasonable prediction method seems to involve theoretical calculations because of the high investment costs of a test building.

Several infiltration and ventilation models have been developed during the last few decades (e.g. by Liddament and Thompson[1], Feustel and Kendon[2], Haghighat[3], and Feustel and Dieris[4]). Most of these programs calculate only the air flow rates (AIRNET[5], MOVECOMP[6], COMIS[7], and DBR-37, LEAKS, SWIFIB, VENT and ELA 4[1,4]), but some comprehensive integrated simulation models (in which the thermal analysis of a building is also included) have also been developed (TARP[8], ESP[9] and PSSP[10]). Most of the simulation programs of both groups still lack the generality of simulating both steady-state and dynamical problems. This is because most of these programs solve only the mass balance equations, and usually ignore the momentum equation. In such cases time-dependent problems cannot be calculated reliably. In this paper a new solution method of air flow and pressure distribution in a building (based on the previous work of Patankar[11], Juslin and Siikonen[12] and Tuomaala[13]) is described.

2 Methods

In this work a ventilation process is modelled by a network. The nodes are connected to each other by one-dimensional flow elements. The improved SIMPLE algorithm (developed by Juslin and Siikonen[12]) is selected to solve the mass balance equations of every node, and the momentum equations of each flow element. These equations are linearised and solved iteratively using a fully implicit method.

2.1 *A solution method for the air flow rates*

An improved SIMPLE algorithm (developed by Patankar[11], and Juslin and Siikonen[12]) is used to calculate mass flow rates between nodes, and pressure distribution inside a building. The solution method is based on simultaneous iterative solution of both the mass balance equation of each node in the network, and the momentum equation of every flow element.

The mass balance equation for every node is:

$$V_i \frac{\mathrm{d}\rho_i}{\mathrm{d}t} + \sum_j \dot{m}_{ij} = S_i \tag{1}$$

and if the mass flow is assumed to be one-dimensional, the momentum equation can be expressed as:

$$\frac{L_{ij}}{A_{ij}} \frac{\mathrm{d}\dot{m}_{ij}}{\mathrm{d}t} - p_i + p_j + \tfrac{1}{2}K_{ij}|\dot{m}_{ij}|\dot{m}_{ij} = S_{ij} \tag{2}$$

where K_{ij} is the dynamic pressure loss coefficient. Derivation of this coefficient from the general momentum equation is presented in Appendix 1. A relationship between a pressure difference across a single flow element and mass flow rate through it is non-linear (except for the ideal laminar flow). Because of this non-linearity of the momentum equation, the solution has to be made iteratively. Juslin and Siikonen[12] have tested several linearisation formulations for the momentum equation, and among different possibilities the following (the derivation of which is presented in Appendix 2) was the optimal one:

$$\begin{aligned}\frac{L_{ij}}{A_{ij}} \frac{\dot{m}_{ij}^{(k)} - \dot{m}_{ij}^{t-\Delta t}}{\Delta t} - p_i^{(k)} + p_j^{(k)} \\ + \tfrac{1}{2}K_{ij}^{(k-1)}|\dot{m}_{ij}^{(k-1)}|\dot{m}_{ij}^{(k-1)} \\ + K_{ij}^{(k+1)}|\dot{m}_{ij}^{(k-1)}|[\dot{m}_{ij}^{(k)} - \dot{m}_{ij}^{(k-1)}] = S_{ij}^{(k-1)}\end{aligned} \tag{3}$$

Superscript $t - \Delta t$ in equation 3 refers to already-known values at a previous moment in time; k refers to new values, and $k - 1$ refers to values during the previous iteration loop.

Pressure losses in the flow elements are often quite small compared with the absolute pressures of the air (1–100 Pa versus 100 000 Pa). Therefore, in order to get more exact calculation results, in the numerical sense, it is more convenient to calculate pressure corrections and mass flow rate corrections (Δp_i and Δm_{ij}) during every iteration step instead of calculating the absolute values for pressures and mass flow rates. In this way the new mass flow rates and the pressures (upper index k) can be calculated from the values of the previous iteration loop (upper index $k - 1$) and the corrections, and they can be written as:

$$\dot{m}_{ij}^{(k)} = \dot{m}_{ij}^{(k-1)} + \Delta\dot{m}_{ij} \tag{4a}$$

$$p_i^{(k)} = p_i^{(k-1)} + \Delta p_i \tag{4b}$$

Residual R_{ij}^m of the momentum equation for flow elements is defined as:

$$\begin{aligned}R_{ij}^m = -\frac{L_{ij}}{A_{ij}} \frac{\dot{m}_{ij}^{(k)} - \dot{m}_{ij}^{t-\Delta t}}{\Delta t} + p_i^{(k)} - p_j^{(k)} \\ - \tfrac{1}{2}K_{ij}^{(k-1)}|\dot{m}_{ij}^{(k-1)}|\dot{m}_{ij}^{(k-1)} \\ - K_{ij}^{(k-1)}|\dot{m}_{ij}^{(k-1)}|(\dot{m}_{ij}^{(k)} - \dot{m}_{ij}^{(k-1)}) + S_{ij}^{(k-1)}\end{aligned} \tag{5}$$

The mass balance equation is numerically solved from:

$$V_i \frac{\rho_i^{(k-1)} - \rho_i^{(t-\Delta t)}}{\Delta t} + V_i \frac{\partial\rho}{\partial p} \frac{1}{\Delta t} \Delta p_i + \sum_j \dot{m}_{ij}^{(k)} = S_i \tag{6}$$

By substituting equation 4a into equation (6), we can obtain:

$$\begin{aligned}V_i \frac{\partial\rho}{\partial p} \frac{1}{\Delta t} \Delta p_i + \sum_j \Delta\dot{m}_{ij} = -V_i \frac{\rho_i^{(k-1)} - \rho_i^{t-\Delta t}}{\Delta t} \\ - \sum_j \dot{m}_{ij}^{(k)} + S_i = R_i\end{aligned} \tag{7}$$

where R_i is the mass flow residual at node i. If we put equations 4a and 4b to the discretised momentum equation 3, the correction of mass flow rate can be written as:

$$\Delta\dot{m}_{ij} = \frac{\Delta p_i - \Delta p_j}{a'_{ij}} + b'_{ij} \tag{8}$$

By introducing to equation 7, the pressure corrections can be expressed as a Poisson type of equation:

$$a_{ii}\Delta p_i = \sum_j a_{ij}\Delta p_i - b_i \tag{9}$$

where

$$a_{ij} = \frac{1}{a'_{ij}}$$

$$a_{ii} = \sum_j \frac{1}{a'_{ij}} + V_i \frac{\partial \rho}{\partial p}\frac{1}{\Delta t}$$

$$b_i = \sum_j b'_{ij} + R_i$$

$$a'_{ij} = \frac{L_{ij}}{A_{ij}}\frac{1}{\Delta t} + K_{ij}^{(k-1)}|\dot{m}_{ij}^{(k-1)}|$$

$$b'_{ij} = R^m_{ij}/a'_{ij} \tag{10}$$

After this, the mass flow rates can be calculated using equation 8. Iteration of pressure corrections and mass flow rate corrections for each time step is continued until the residuals of mass balance equations and momentum equations are small enough (maximum mass flow rate and momentum equation residuals are, for example, less than 0.001 kg s^{-1} and 0.1 Pa). When the convergence criteria is fulfilled, the pressures and mass flow rates for the next time step can be solved.

Assumptions made here are that the flow area A_{ij} and the velocity along a single flow element are constants, which means that inlet and outlet velocities are equal. Also air density through a flow element is assumed to be constant.

2.2 *Models of the driving forces*

In the present version of the simulation program (BUS version 2.1), the wind effect and the stack effect (caused by the differences in densities and heights) are included as driving forces of air movement between nodes. Modelling of fans has not yet been tested properly, but it is planned to incorporate it into the next version of the program.

Wind pressure is present at the external nodes of the whole system. Therefore, these pressure differences at the external nodes are calculated by the equation:

$$\Delta p_{\text{wind}} = C_p 0.5 \rho v^2_{\text{wind}} \tag{11}$$

and here these pressure differences are assumed to be constants during each time step.

The stack effect is included in every node of the system by the equation:

$$\Delta p_{\text{stack}} = -S_{ij} = g\{\rho_i h_i + \rho_{ij}[(z_j + h_j) - (z_i + h_i)] - \rho_i h_i\} \tag{12}$$

where z is the node level from the reference, h is the height of an opening from the node level, and ρ is density. The stack effect is calculated and included in the source term S_{ij} of the momentum equation for every flow element of the process (Figure 1).

It is planned that fans, as the source of the pressure difference, will be approximated in the next version of the program by polynomial equations:

$$\Delta p_{\text{fan}} = s_0 + s_1 \dot{V}_{ij} + s_2 \dot{V}^2_{ij} + s_3 \dot{V}^3_{ij} \tag{13}$$

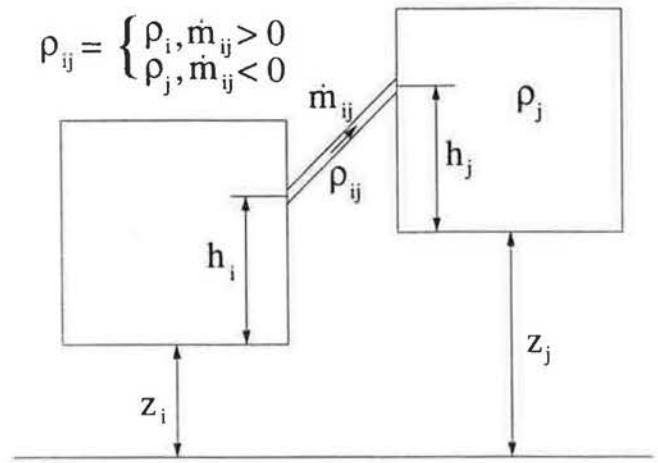

Figure 1 Stack effect and variable definition

where parameters s_0, s_1, s_2, and s_3 are constants of a fan-specific curve.

2.3 *Defining the behaviour of flow elements*

As mentioned earlier—and presented in Appendix 1—the relationship between a pressure difference across a flow element and mass flow rate through it is approximated by a general expression:

$$\Delta p = \tfrac{1}{2} K_{ij} |\dot{m}_{ij}| \dot{m}_{ij} \tag{14}$$

This is done in order to get as general a formulation for the momentum equation as possible. (The more general the formulation, the simpler the linearisation of the equation, and the more effective the program.) For each flow element the approximative value of the individual dynamic pressure loss coefficient K_{ij} is defined for every iteration loop, since the values of these coefficients depend on both the constant parameter values of each type of flow element (presented in Appendix 3), and the process variables (e.g. mass flow rates). When a discretised solution method is used—as in this simulation model—the steady-state flow forms of pressure loss coefficients (equation 14) remain valid dynamic simulations. This is because the dynamic behaviour of a single flow element is approximated by the flow dimensions and time derivative of mass flow rate (presented in the momentum equation, equation 2, earlier) only, and at a discretised time point the updated value of K_{ij} approximates the behaviour of a flow element.

2.4 *Process description*

A ventilation process to be simulated has to be described unambiguously for a simulation program. The present version of this simulation program (BUS version 2.1) requires the following three input data files:

- input data file of the process to be simulated
- wind pressure coefficient data for wind effect calculation
- outdoor weather input data file.

The *process input data file* includes:

(*a*) the general data about the process
(*b*) the data about nodes inside and the building

(*c*) the data about the flow elements between all nodes.

The general process data (*a*) include the total number of nodes, the number of external nodes, time step, and convergence criteria for both mass balance equations and momentum equations. The initial values of pressure, volume, height from the neutral level and constant temperature are given as node input data (see (*b*)). Several flow element types (i.e. approximations of their flow equation) are included in the model (duct element, quadratic flow element, power law flow element and damper element). Flow element input data include numbers of starting and ending nodes, flow element type, height values of a flow element compared with floor level of connected nodes, and initial residual momentum equation (see (*c*)). Mathematical formulations of these approximations of the flow element types are presented in Appendix 1. An example of the process input data file is presented in Appendix 4.

The *wind pressure coefficient data file* includes the coefficient values of all outdoor nodes for eight wind directions (starting from North continuing in steps at 15° clockwise). In the *weather input data file* outdoor air pressure, temperature, wind direction and wind velocity are presented.

3 A numerical example

A test case of air infiltration similar to that of Haghighat and Rao[14] is used. In Figure 2 this air infiltration process (including the height values of the different levels of the rooms and flow elements) is shown. The power law flow elements are selected, and in Table 1 the parameter values for every flow element are presented.

Table 2 Wind pressures for external nodes, and temperatures of every node of a test case called FLOW TEST 1

Node number	Temperature (°C)	Wind pressure (Pa)
1	0.0	—†
2	0.0	11.0
3	0.0	3.7
4	0.0	−7.3
5	0.0	−4.9
6	23.0	—
7	21.0	—
8	23.0	—
9	21.0	—

† Reference point at ground level (p_{ref} = 101 325.0 Pa)

In Table 2 the wind pressures for external nodes, and temperatures of every node of the test case called FLOW TEST 1, are presented. A reference pressure of 101 325.0 Pa at ground level is used. The moisture content of the air everywhere in the process is equal to zero. The test case is simulated using initial pressure values of 101 325.0 Pa for every internal node, a time step of 60.0 s, and $[\max(|R_i|)] < 0.0001\,\mathrm{kg\,s^{-1}}$ and $[\max(|R_{ij}^m|)] < 0.01$ Pa as convergence criteria for maximum residuals of mass balance and momentum equations.

In Table 3 the simulated steady-state node pressures, and pressure differences between node pressure and reference pressure outside a building at ground level are presented; in Table 4 the simulated and calculated steady-state mass flow rates, relative differences between simulated and calculated mass flow rates, and source

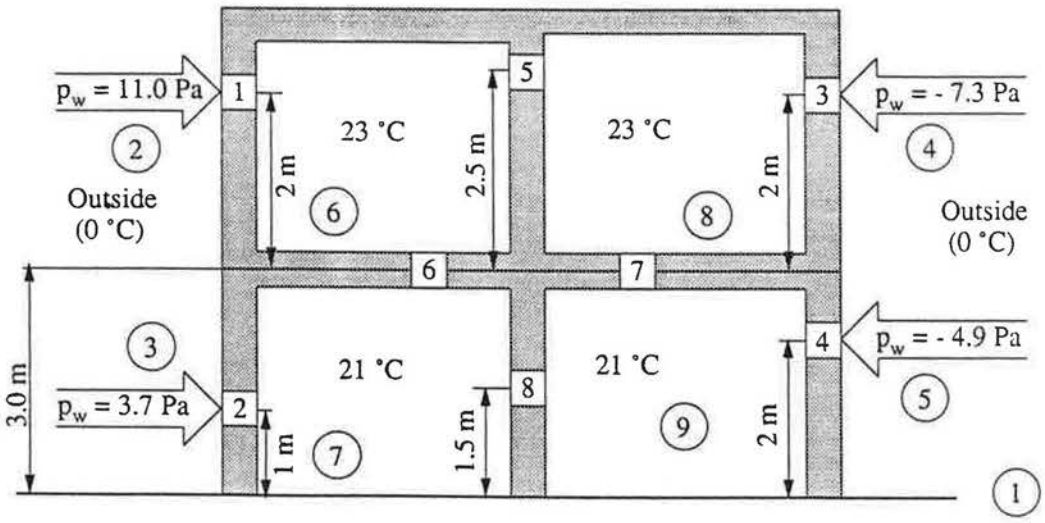

Figure 2 A four-room building of the second numerical example. Node numbers are inside the circles, and flow element numbers are inside the squares.

Table 1 Flow element parameters of a test case called FLOW TEST 1

Flow element number	C_{plc} ($m^3\,s^{-1}\,Pa^{-0.65}$)	n	Flow element number	C_{plc} ($m^3\,s^{-1}\,Pa^{-0.5}$)	n
1	0.005	0.65	5	0.015	0.5
2	0.008	0.65	6	0.020	0.5
3	0.007	0.65	7	0.020	0.5
4	0.009	0.65	8	0.015	0.5

Table 3 Simulated steady-state node pressures of a test case called FLOW TEST 1

Node number (Pa)	Pressure (Pa)	Pressure difference† (Pa)
1	101 325.00	0.00
2	101 336.00	11.00
3	102 328.70	3.70
4	101 317.70	−7.30
5	101 320.10	−4.90
6	101 287.88	−37.12
7	101 323.20	−1.80
8	101 285.67	−39.33
9	101 321.04	−3.96

† Pressure difference compared with reference pressure 101 325.0 Pa at node number 1

terms of a test case called FLOW TEST 1 are presented. The calculated mass flow rates are obtained by using simulated node pressures and input parameter data of flow elements. The maximum relative difference between calculated and simulated mass flow rates was 5.1% in flow element number 6. (This is the flow element between the two rooms situated one above the other on the windward side.) Here, the absolute difference is very small ($8.0 \times 10^{-5}\,kg\,s^{-1}$), and it could be reduced if more iterations were performed. The average value of the relative difference between simulated and calculated mass flow rates (initial values mentioned above) was 0.90% and, according to these comparisons, the results given by this new solution method for an air infiltration and ventilation model are reliable.

The convergence of the solution method is tested by using three different initial mass flow rate values of the simulation:

(*a*) realistic initial mass flow rate values for each flow element (paying attention to both magnitude and direction of the mass flow)
(*b*) constant mass flow rate values of $0.001\,kg\,s^{-1}$
(*c*) constant mass flow rate values of $0.1\,kg\,s^{-1}$.

Here the convergence of the solution method is estimated by the maximum residual of the flow element momentum equations. Figure 3 shows these maximum residuals

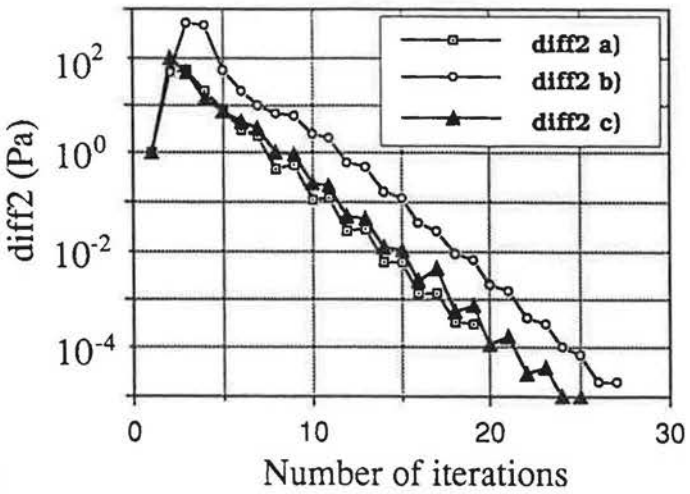

Figure 3 The maximum residuals (diff2) of flow element momentum equations as a function of iteration loops, when three different initial mass flow rate values (cases (*a*), (*b*) and (*c*) defined in the text) are used

(diff2) in three simulated cases on a logarithmic scale. When the simple air flow test case (defined above) is simulated by the solution method studied, the values of the maximum residual decrease by about five orders of magnitude during 15 iteration loops; this means, on average, one order of magnitude in three iteration loops, which seems quite promising.

4 Discussion and future outlook

The development of single-zone models seems to be completed. The development of multi-zone infiltration and ventilation models shows evolution. Lack of exchange of information, restricted distribution of models and lack of a flexible structure are probably the reasons why models developed in the early seventies are not very different from those in the late eighties[15].

Although the simplest tests of the present simulation programs look very promising, some important questions remain. The most impotant question concerns the reliability of the method for solving air flow network equations. Solution of the non-linear equations has been

Table 4 Simulated and calculated steady-state mass flow rates, relative differences between simulated and calculated mass flow rates, and source terms of a test case called FLOW TEST 1

Flow element number	Mass flow rate		Relative difference between simulated and calculated mass flow rates†	Buoyancy source term (Pa)
	Simulated ($kg\,s^{-1}$)	Calculated ($kg\,s^{-1}$)		
1	0.025 14	0.025 18	−0.001 518	40.016
2	0.027 89	0.027 85	0.001 302	0.906
3	−0.032 15	−0.032 16	−0.000 349	40.006
4	−0.020 88	−0.020 84	0.001 735	1.810
5	0.026 57	0.026 54	0.000 953	0.001
6	−0.001 43	−0.001 51	−0.051 161	−35.316
7	−0.005 58	−0.005 63	−0.008 242	−35.315
8	0.026 46	0.026 28	0.007 017	0.000

† Relative differences have been calculated using the equation:

$$\frac{\dot{m}_{simulated} - \dot{m}_{calculated}}{\dot{m}_{calculated}}$$

demonstrated in several tests but has not been mathematically proven[5].

When developing the next version of this building simulation model (BUS), it is planned to include a sub-model of thermal analysis of a building. The assembly of the flow components should also be enlarged, and typical combinations of parameter values for different flow elements will be defined. In the future work, the simulation program will also involve indoor air quality simulation.

According to this study the new solution method of a multi-zone air infiltraton and ventilation simulation model is promising. Maybe the main benefit of this solution method is that it also allows a program end-user to study time-dependent ventilation processes. The other benefit of this method is the stability of the solution algorithm. The solution method has, however, been tested using a simple test case only. Therefore, more complex test cases need to be simulated in order to validate the simulation model properly.

Acknowledgements

Professors Ilmari Kurki-Suonio and Markku Lampinen have both encouraged me in my postgraduate studies. This paper is the result of fruitful discussions with them, and I therefore wish to thank them both very warmly for the constructive criticism and support I have received while writing it.

Special thanks are due to Dr Timo Siikonen, for providing me with fundamental ideas and theoretical tools to develop this air flow simulation model. Last, but not least, I wish to thank Mrs Elizabeth Heap-Talvela for encouraging me to write this paper and checking the text.

References

1 Liddament M and Thompson C *Mathematical models of air infiltration—a brief review and bibliography* Technical Note **AIC 9** (Bracknell: Air Infilatration Centre) (1982)
2 Feustel H E and Kendon V M Infiltration models for multicellular structures—a literature review *Energy and Buildings* **8**(2) 123–136 (1985)
3 Haghighat F Air infiltration and indoor air quality models—a review *Int. J. Ambient Energy* **10**(3) 115–122 (1989)
4 Feustel H E and Dieris J A Survey of airflow models for multizone structures *Energy and Buildings* **18**(2) 79–100 (1992)
5 Walton G N *AIRNET—a computer program for building airflow network modelling* **NISTIR 89-4072** (Gaithersburg MD: National Institute of Standards and Technology) (1989)
6 Herrlin M K MOVECOMP: A static-multicell-airflow-model *ASHRAE Trans.* **91** Part 2B HI-85-40 1989–1996 (1985)
7 Feustel H E and Raynor-Hoosen A *Fundamentals of the multizone air flow model—COMIS* Technical Note **AIVC 29** (Coventry: Air Infiltration and Ventilation Centre) (1990)
8 Walton G N Airflow and multiroom thermal analysis *ASHRAE Trans.* **88**(2704) 78–90 (1982)
9 Clarke J *Energy simulation in building design* (Bristol: Adam Hilger) (1985)
10 Hayashi T, Urano Y, Katayama T, Sugai T, Watanabe T, Shiotuki Y and Zhang Q Prediction of air distribution in multiroom buildings *Proc. Roomvent '87 Air distribution in ventilated spaces Session 4b, Stockholm, Sweden* (10–12 June 1987)
11 Patankar S V *Numerical heat trnasfer and fluid flow* (New York: McGraw-Hill) (1980)
12 Juslin K and Siikonen T Solution methods for pipe network analysis *IAEA/NPPC/Specialists' Meeting on Nuclear Power Plant Training Simulators, Otaniemi, Finland* (12–14 September 1983)
13 Tuomaala P *Numerical simulation model for building air flows and air quality* Licentiate thesis, Helsinki University of Technology (in Finnish) (1990)
14 Haghighat F and Rao J Computer-aided building ventilation system design—a system-theoretic approach *Energy and Buildings* 17(2) 147–155 (1991)
15 Feustel H E Mathematical modelling of infiltration and ventilation *10th AIVC Conference, Dipoli, Finland* pp 121–141 (25–28 September 1989)

Appendix 1: Derivation of dynamic pressure loss coefficient (K_{ij}) from general momentum equation

The general momentum equation can be expressed[11]:

$$\frac{\partial}{\partial t}(\rho u) + \mathrm{div}(\rho \boldsymbol{u} u) = \mathrm{div}(\mu\ \mathrm{grad}\ u) - \frac{\partial p}{\partial x} + B_x + V_x \tag{15}$$

where u denotes the x-direction velocity, μ is the viscosity, p is the pressure, B_x is the x-direction body force per unit volume, and V_x stands for the viscous terms that are in addition to those expressed by $\mathrm{div}(\mu\ \mathrm{grad}\ u)$. Equation 15 can be simplified as[12]:

$$\frac{L_{ij}}{A_{ij}}\frac{\mathrm{d}\dot{m}_{ij}}{\mathrm{d}t} - p_i + p_j + \tfrac{1}{2}K_{ij}|\dot{m}_{ij}|\dot{m}_{ij} = S_{ij} \tag{16}$$

The assumptions made here are that the flow area A_{ij} and the velocity along a single flow element are constants, which means that inlet and outlet velocities are equal. Also air density through a flow element is assumed to be constant. The first term of equation 16 represents the changing rate of the mass flow rate through a flow element, and it approximates the unsteady behaviour of a flow element. Pressures p_i and p_j come from the pressure gradient $\partial p/\partial x$ in equation 15. The second term of equation 15 is missing from equation 16, because velocity in the x-direction is assumed to be constant. The right-hand side variable S_{ij} of equation 16 is a pressure source in the flow element between nodes i and j, including the stack effect defined in section 2.2 and pressure difference generated by a fan.

All the viscous forces in equation 15 are included in the term:

$$\tfrac{1}{2}K_{ij}|\dot{m}_{ij}|\dot{m}_{ij}$$

where K_{ij} is called dynamic pressure loss coefficient. This coefficient can be defined in steady state conditions in a laboratory. Several fittings for various flow element types can be presented. In Appendix 3 the flow element approximations used in the present version of this simulation program (BUS version 2.1) are presented.

Appendix 2: Derivation of discretisation of general momentum equation

The discretisation of the momentum equation

$$\frac{L_{ij}}{A_{ij}}\frac{\mathrm{d}\dot{m}_{ij}}{\mathrm{d}t} - p_i + p_j + \tfrac{1}{2}K_{ij}|\dot{m}_{ij}|\dot{m}_{ij} = S_{ij} \tag{17}$$

can be written as:

$$\frac{L_{ij}}{A_{ij}}\frac{\dot{m}_{ij}^t - \dot{m}_{ij}^{t-\Delta t}}{\Delta t} - p_j^t + p_j^t + \tfrac{1}{2}K_{ij}|\dot{m}_{ij}^t|\dot{m}_{ij}^t = S_{ij} \tag{18}$$

where t is time and Δt is the time step. First, a new mass flow rate of the next time step is written in the form:

$$\dot{m}_{ij}^{t} = \dot{m}_{ij}^{k} = \dot{m}_{ij}^{k-1} + (\dot{m}_{ij}^{k} - \dot{m}_{ij}^{k-1}) \tag{19}$$

and

$$\tfrac{1}{2}(\dot{m}_{ij}^{k})^2 = \dot{m}_{ij}^{k-1}(\dot{m}_{ij}^{k} - \dot{m}_{ij}^{k-1}) + \tfrac{1}{2}(\dot{m}_{ij}^{k-1})^2 + \tfrac{1}{2}(\dot{m}_{ij}^{k} - \dot{m}_{ij}^{k-1})^2 \tag{20}$$

where k is an index of an iteration loop. By neglecting the last term in equation 20, equation 18 can be rewritten as:

$$\frac{L_{ij}}{A_{ij}} \frac{\dot{m}_{ij}^{(k)} - \dot{m}_{ij}^{t-\Delta t}}{\Delta t} - p_i^{(k)} + p_j^{(k)} + \tfrac{1}{2}K_{ij}^{(k-1)} |\dot{m}_{ij}^{(k-1)}| \dot{m}_{ij}^{(k-1)} + K_{ij}^{(k-1)} |\dot{m}_{ij}^{(k-1)}| [\dot{m}_{ij}^{(k)} - \dot{m}_{ij}^{(k-1)}] = S_{ij}^{(k-1)} \tag{21}$$

In the equations above, the superscript $(t - \Delta t)$ refers to already known values at the previous moment in time; k refers to new values, and $k - 1$ refers to values during the previous iteration loop.

Appendix 3: Mathematical approximations of flow element types and dynamic pressure loss coefficients (K_{ij}) of these flow element types

(*a*) Duct element:

$$\Delta p = \lambda \frac{L}{d} \frac{1}{2} \rho v^2$$

$$K_{ij}^{(k-1)} = \frac{16 \lambda_{ij} L_{ij}}{\pi^2 d_{ij}^5 \rho_{ij}}$$

(*b*) Quadratic flow element:

$$\Delta p = a_{\text{quadr}} \dot{V}_{ij} + b_{\text{quadr}} \dot{V}_{ij}^2$$

$$K_{ij}^{(k-1)} = \frac{2a_{\text{quadr}}}{\rho_{ij} \dot{m}_{ij}} + \frac{2b_{\text{quadr}}}{\rho_{ij}^2}$$

(*c*) Power law flow element:

$$\dot{V}_{ij} = C_{\text{plc}} \Delta p^n$$

$$K_{ij}^{(k-1)} = \frac{2}{(C_{\text{plc}} \rho_{ij})^{1/n}} \dot{m}_{ij}^{[(1/n)-2]}$$

(*d*) Damper element (δ is opening angle of damper plates (°)):

$$\Delta p = \zeta \tfrac{1}{2} \rho_{ij} v_{ij}^2$$

$$\zeta = 2000 \times 10^{(\exp(-\delta/4) - 0.0436\delta)}$$

$$K_{ij}^{(k-1)} = \frac{16\zeta}{\pi^2 d_{ij}^4 \rho_{ij}}$$

Appendix 4: Example of an input data file

General data: number of nodes, external nodes, simulation time, time at the beginning, time step

```
9    5    3600.0    0.0    600.0
```

Node data: pressure, volume, level and temperature data

```
101325.0    75.0    3.0    23.0
101325.0    75.0    0.0    21.0
101325.0    75.0    3.0    23.0
101325.0    75.0    0.0    21.0
```

Flow element data, the first line: starting node, ending node, mass flow rate, flow element type (4 means exponential flow element), heights of the flow element from node levels of connecting nodes, and initial momentum residual

```
2    6    0.010    4    5.0    2.0    0.001
```

Flow element data, the second line (for exponential flow element!): ratio between length and flow area of a flow element, coefficient, exponent

```
1.0    0.005    0.65
```

Rest of the flow element data as defined above

```
3    7    0.032    4    1.0    1.0    0.001
1.0       0.008    0.65
4    8    -0.002   4    5.0    2.0    0.001
1.0       0.007    0.65
5    9    -0.040   4    2.0    2.0    0.001
1.0       0.009    0.65
6    8    0.018    4    2.5    2.5    0.001
1.0       0.015    0.5
6    7    -0.008   4    0.0    3.0    0.001
1.0       0.020    0.5
8    9    0.015    4    0.0    3.0    0.001
1.0       0.020    0.5
7    9    0.024    4    1.5    1.5    0.001
1.0       0.015    0.5
```